Development 136, 2601-2611 (2009) doi:10.1242/dev.038315

Zebrafish mutations in *gart* and *paics* identify crucial roles for de novo purine synthesis in vertebrate pigmentation and ocular development

Anthony Ng[1], Rosa A. Uribe[1], Leah Yieh[1], Richard Nuckels[1] and Jeffrey M. Gross[1,2,*]

Although purines and purinergic signaling are crucial for numerous biochemical and cellular processes, their functions during vertebrate embryonic development have not been well characterized. We analyze two recessive zebrafish mutations that affect de novo purine synthesis, *gart* and *paics*. *gart* encodes phosphoribosylglycinamide formyltransferase, phosphoribosylglycinamide synthetase, phosphoribosylaminoimidazole synthetase, a trifunctional enzyme that catalyzes steps 2, 3 and 5 of inosine monophosphate (IMP) synthesis. *paics* encodes phosphoribosylaminoimidazole carboxylase, phosphoribosylaminoimidazole succinocarboxamide synthetase, a bifunctional enzyme that catalyzes steps 6 and 7 of this process. Zygotic *gart* and *paics* mutants have pigmentation defects in which xanthophore and iridophore pigmentation is almost completely absent, and melanin-derived pigmentation is significantly decreased, even though pigment cells are present in normal amounts and distributions. Zygotic *gart* and *paics* mutants are also microphthalmic, resulting from defects in cell cycle exit of proliferative retinoblasts within the developing eye. Maternal-zygotic and maternal-effect mutants demonstrate a crucial requirement for maternally derived *gart* and *paics*; these mutants show more severe developmental defects than their zygotic counterparts. Pigmentation and eye growth phenotypes in zygotic *gart* and *paics* mutants can be ascribed to separable biosynthetic pathways: pigmentation defects and microphthalmia result from deficiencies in a GTP synthesis pathway and an ATP synthesis pathway, respectively. In the absence of ATP pathway activity, S phase of proliferative retinoblasts is prolonged and cell cycle exit is compromised, which results in microphthalmia. These results demonstrate crucial maternal and zygotic requirements for de novo purine synthesis during vertebrate embryonic development, and identify independent functions for ATP and GTP pathways in mediating eye growth and pigmentation, respectively.

KEY WORDS: De novo purine synthesis, Microphthalmia, Pigmentation, Zebrafish

INTRODUCTION

Purines can be generated de novo or they can be recycled from sources within the body through a 'salvage pathway' (Zalkin and Dixon, 1992; Zollner, 1982). De novo synthesis starts with the precursor 5-phospho-D-ribosyl-1-pyrophosphate (PRPP) and this is converted to inosine monophosphate (IMP) through ten enzymatic steps (Fig. 1). IMP then feeds into pathways leading to AMP and GMP formation, and these serve as precursors for their high energy di- or tri-phosphate forms (the 'ATP pathway' and the 'GTP pathway').

Although much work has been performed to identify the biochemical mechanisms underlying de novo purine biosynthesis in prokaryotic and eukaryotic systems (Zalkin and Dixon, 1992), the role that purines and purinergic signaling play during embryonic development in animals has not been well characterized. Perhaps the most well-studied model for the function of the de novo purine synthesis pathway during development comes from work in *Drosophila*, in which mutations in *prat* (*ppat*) (Clark, 1994), *ade2* (*pfas*) (Henikoff et al., 1986b; Johnstone et al., 1985), *ade3* (*gart*) (Henikoff et al., 1986a; Johnstone et al., 1985) and *ade5* (*paics*) (O'Donnell et al., 2000) have been identified, as well as mutations in the GTP pathway components *IMPDH* (*raspberry*) and *GMP synthase* (*burgundy*) (Johnstone et al., 1985; Long et al., 2006). Each of these de novo pathway mutants shows a subset of developmental defects that have collectively been termed the 'purine syndrome' phenotype (Tiong et al., 1989). Purine syndrome defects include a reduction in the red pteridine-derived eye pigments, bristle and leg malformations, small wings, and pupal lethality (Tiong et al., 1989). Additionally, *IMPDH* and *GMP synthase* mutants possess defects in R-cell axon pathfinding (Long et al., 2006).

Developmental roles for the de novo purine synthesis pathway in vertebrates have been elusive, however, purinergic signaling is known to have several functions during vertebrate embryonic development. Recent studies have highlighted a crucial role for retinal pigmented epithelium (RPE)-released ATP in regulating retinoblast proliferation (Martins and Pearson, 2008; Pearson et al., 2002; Pearson et al., 2005). Moreover, E-NTPDase2, an enzyme that converts ATP to ADP, has been shown to function in eye formation upstream of the eye field transcription factor network (Massé et al., 2007). Additionally, GTP is thought to serve as the precursor for the formation of each of the pigment types in the zebrafish embryo (Ziegler, 2003). Although these studies highlight important developmental roles for purine nucleotides or their products, how the de novo pathway itself functions during vertebrate embryonic development remains unclear.

With an interest in this pathway, we have characterized two recessive zebrafish mutations that affect de novo purine synthesis, *gart* and *paics* (Amsterdam et al., 2004; Gross et al., 2005). *gart* encodes a trifunctional enzyme that catalyzes steps 2, 3 and 5 of IMP synthesis, and *paics* encodes a bifunctional enzyme that catalyzes steps 6 and 7 of this process (Fig. 1). *gart* and *paics* mutants are microphthalmic and they possess pigmentation defects that affect each of the pigment cell types of the embryo: the melanin-containing

[1]Section of Molecular Cell and Developmental Biology, Institute for Cell and Molecular Biology and [2]Institute for Neuroscience, The University of Texas at Austin, Austin, TX 78722, USA.

*Author for correspondence (e-mail: jmgross@mail.utexas.edu)

Accepted 26 May 2009

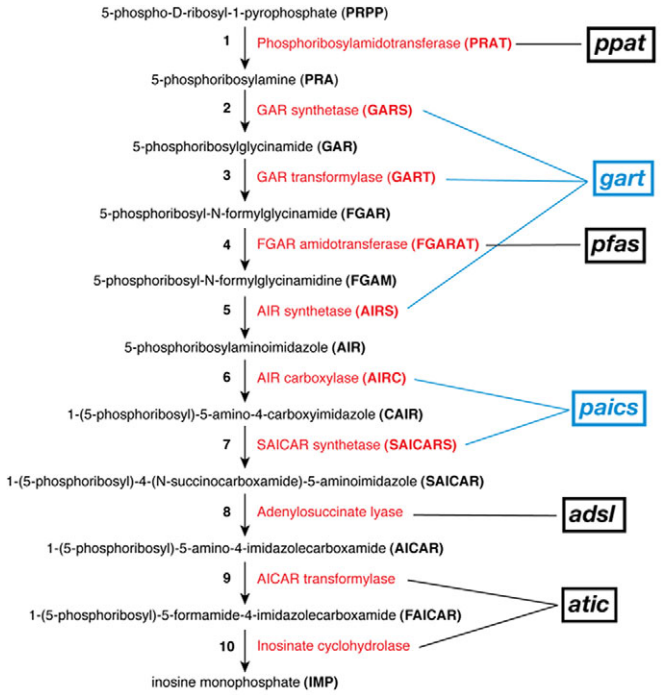

Fig. 1. The de novo purine synthesis pathway. Synthesis of IMP, the precursor for AMP and GMP, proceeds through ten enzymatic steps. Black, precursor molecule and acronym; red, enzyme that catalyzes its conversion and eukaryotic acronym; boxes, zebrafish genes encoding these enzymatic functions.

melanosomes in skin melanocytes and the RPE; the guanine stack-containing iridosomes in iridophores; and the pteridine-containing pterinosomes in xanthophores. Utilizing *gart* and *paics* mutants, and morpholino knockdown of components unique to the ATP or GTP pathways, we present data supporting a model in which an ATP pathway is required for eye growth, and a GTP pathway is required for pigmentation.

MATERIALS AND METHODS

Zebrafish maintenance and mutant alleles

Zebrafish (*Danio rerio*) adults and embryos were maintained at 28.5°C on a 14-hour light/10-hour dark cycle. Animals were treated in accordance with the University of Texas at Austin provisions governing animal use and care. Mutant alleles used in this study were *paics*^{hi2688}, *gart*^{hi3526b} and *adssl*^{hi3081}.

RT-PCR

Embryos (10-20) were homogenized in TRIzol Reagent (Invitrogen) using a 25-gauge needle. Total RNA was purified by chloroform extraction and isopropanol precipitation. cDNA was synthesized from 500 ng of total RNA using an iScript cDNA Synthesis Kit (BioRad). PCR was performed using 1.25 μL of cDNA. Primer sequences are available upon request.

Histology

Histology was performed as described in Nuckels and Gross (Nuckels and Gross, 2007).

Transmission electron microscopy (TEM)

Embryos were processed for histology and transverse 70-90 nm sections were cut through the central retina and mounted onto grids. Sections were stained with lead citrate and uranyl acetate. Images were obtained on a Philips EM 208 transmission electron microscope (80 kV) via an AMT Advantage HR 1MB digital camera. Images were processed using Adobe Photoshop CS2.

Riboprobes and in situ hybridization

Hybridizations were performed essentially as described by Jowett and Lettice (Jowett and Lettice, 1994). cDNA clones encoding *PNPase*, *gch* and *dct* were provided by David Parichy (University of Washington, Seattle, WA, USA) and those encoding *ccnd1* and *ccnb1* were purchased from ZIRC (Eugene, OR, USA).

Melanin quantification assay

Melanin quantification was performed as described in Maldonado et al. (Maldonado et al., 2006). At least 20 embryos were analyzed per trial, and 2-6 trials were performed using different clutches of embryos. The data were graphed and statistical significance was calculated using a Student's *t*-test (GraphPad Prism).

Immunohistochemistry

Immunohistochemistry was performed as described in Uribe and Gross (Uribe and Gross, 2007). The following antibodies and dilutions were used: zpr1 (1:200); zn8 (1:100); zpr2 (1:200); and goat anti-mouse Cy3 secondary (1:500). Imaging was performed on a Zeiss LSM5 Pascal laser scanning confocal microscope.

BrdU assays

BrdU incorporation assays were performed as described in Lee et al. (Lee et al., 2008). Cell counts were performed on sections through the central retina. $BrdU^+$ nuclei were counted from sections obtained from three to five different embryos, derived from at least two different mating pairs. Averages of $BrdU^+$ cells were compared with wild-type controls using a Student's *t*-test for statistical significance (GraphPad Prism).

TUNEL assays

TUNEL assays were performed on cryosections using a TMR red in situ cell death detection kit (Roche) and were imaged by confocal microscopy.

Morpholino injections and RT-PCR

adss, gmps and standard control morpholinos (MOs) were purchased from Gene Tools (Philomath, OR, USA): adss-MO, 5′-TCCAC-CCTGCACAAACACTGACGTT-3′; gmps-MO, 5′-CACCTACTGAC-AGTGCTCACCTGAA-3′; and were injected into Oregon AB embryos. Splicing alterations were verified by RT-PCR and DNA sequencing.

Flow cytometry

FACS analysis was performed as in Bessa et al. (Bessa et al., 2008). DNA content was analyzed on a BD FACSCalibur flow cytometer using at least 25,000 cells/condition. Data analysis was performed using FlowJo software and statistical analysis was performed using a two parametric, unpaired *t*-test (GraphPad Prism).

RESULTS

gart and *paics* mutants possess pigmentation defects and are microphthalmic

Homozygous *gart* and *paics* mutant embryos possess pigmentation defects in which nearly all xanthophore-derived yellow pigmentation and iridophore-derived silver/reflective pigmentation is absent (Fig. 2). Melanophore/RPE-derived black pigmentation is present but embryos appeared lighter than their wild-type siblings. This lighter appearance could result from decreases in overall melanin levels, or from defects in melanosome distribution within mutant pigment cells. To differentiate between these possibilities we utilized a biochemical purification method to quantify melanin levels at 3.5 dpf and 5 dpf (Maldonado et al., 2006). At both times, *gart* and *paics* mutants possessed significantly less melanin (see Fig. S1 in the supplementary material).

In addition to pigmentation defects, *gart* and *paics* mutants were also microphthalmic (Fig. 2; Table 1). *paics* mutants were first phenotypically identifiable at 48 hpf. Histologically, the *paics* mutant eye was dramatically smaller than that of a wild-type sibling, and retinal lamination and neuronal differentiation were delayed

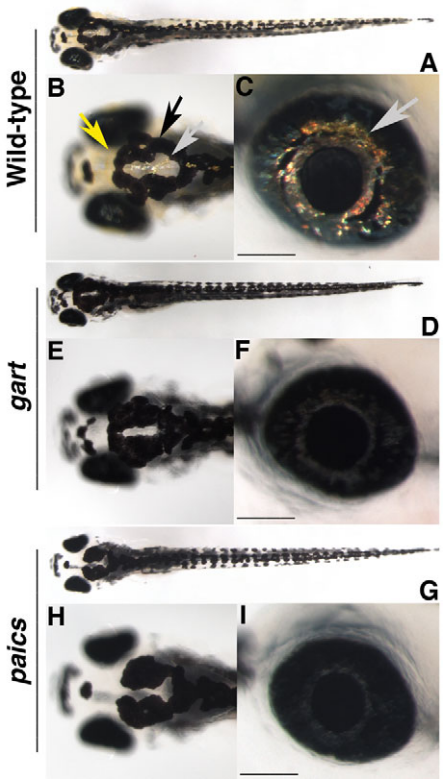

Fig. 2. *gart* and *paics* mutants have pigmentation defects and microphthalmia. (**A-G**) Dorsal (A,B,D,E,G,H) and lateral (C,F,I) images of wild-type (A-C), *gart* (D-F) and *paics* (G-I) embryos at 5 dpf. Wild-type embryos possess xanthophore (yellow arrow), melanophore (black arrow) and iridophore (gray arrow) derived pigments. *gart* and *paics* mutants have substantially less xanthophore and iridophore pigmentation and reduced levels of melanin pigmentation. Mutants are also microphthalmic. Scale bar: 100μm.

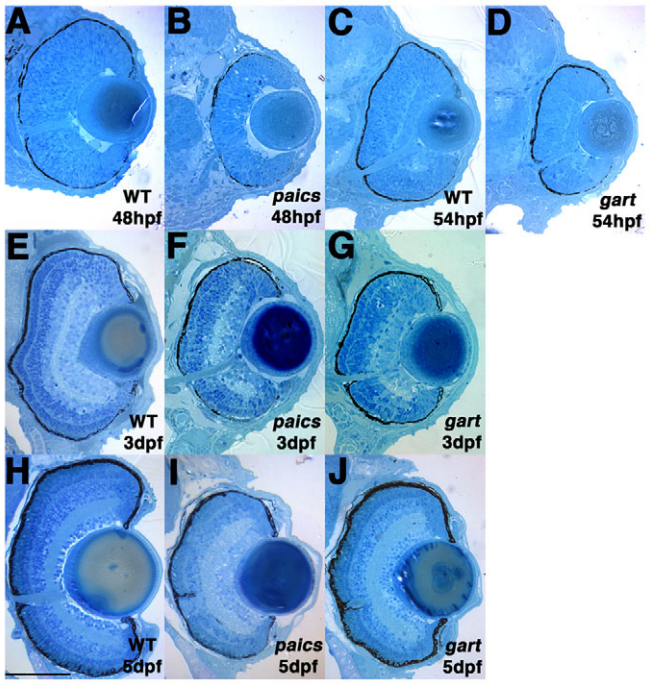

Fig. 3. Histological analysis of *gart* and *paics* mutants. (**A-J**) Transverse histological sections of wild type (A,C,E,H), *gart* (D,G,J) and *paics* (B,F,I) mutants. (A,B) *paics* mutants are identifiable at 48 hpf and are microphthalmic with a hypopigmented RPE. Retinal lamination and neuronal differentiation are also delayed. (C,D) *gart* mutants are morphologically obvious at 54 hpf and are microphthalmic with a hypopigmented RPE. Retinal lamination and neuronal differentiation are also delayed. (E-G) At 72 hpf, mutant eyes remain microphthalmic, however, the retina is well laminated and all cell types appear to be present. (H-J) At 5 dpf, mutant eyes remain microphthalmic. Scale bar: 100 μm. Dorsal is up.

(Fig. 3A,B). *gart* mutants were not identifiable until ~54 hpf and, like *paics* mutants, *gart* mutants also showed delayed retinal lamination and neuronal differentiation (Fig. 3C,D). Both *gart* and *paics* mutants remained microphthalmic at 3 dpf, although retinal lamination and neuronal differentiation appeared to have recovered (Fig. 3E-G). By 5 dpf, the mutant eye had grown considerably but was still smaller than that of wild-type siblings (Fig. 3H-J, Table 1). Lamination was normal and, histologically, all cell types appeared to be present. To confirm this latter point, immunohistochemical analyses were performed: retinal ganglion cells (RGCs) and red/green double cones were present in the mutant retinas (see Fig. S2 in the supplementary material), as well as rods, bipolar cells and amacrine cells (data not shown). RPE differentiation was also unaffected, although in some mutants clumps of morphologically abnormal RPE were occasionally detected (see Fig. S2I in the supplementary material). Examination of RGC axon growth and organization within the optic nerve and optic tract revealed no obvious defects in *gart* and *paics* mutants (data not shown).

Finally, whereas most zygotic *gart* and *paics* mutants were embryonic lethal, we were able to rear ~5-10% of homozygous mutants to adulthood. In these mutants, eye size was normal and pigmentation levels recovered over 1-2 months, at which point the mutants resembled wild-type and heterozygous siblings in their levels of pigmentation (see Fig. S3 in the supplementary material). No additional defects were observed in these fish.

Because *paics* and *gart* mutants were generated through retroviral insertional mutagenesis (Amsterdam et al., 2004; Golling et al., 2002; Gross et al., 2005), we first wanted to determine what effect proviral insertion had on the expression of the locus. In Fig. 4A and Fig. 5A, the approximate position of each proviral insertion has been

Table 1. Eye size measurements at 5 dpf

Genotype	A/P axis	D/V axis	N/T axis
Wild type	304±13.58	257.2±9.11	187.8±6.66
gart	256.1±7.22 P=1.4×10^{-7}	214.2±7.21 P=1.4×10^{-9}	157.9±6.9 P=1.1×10^{-8}
paics	257.3±18.54 P=7.22×10^{-6}	215.6±12.76 P=2.6×10^{-7}	160.2±14.91 P=1.5×10^{-4}

Measurements (in μm) were made along the anterior/posterior (A/P), dorsal/ventral (D/V) and nasal/temporal (N/T) axes of ten embryos and averaged. P values are indicated.

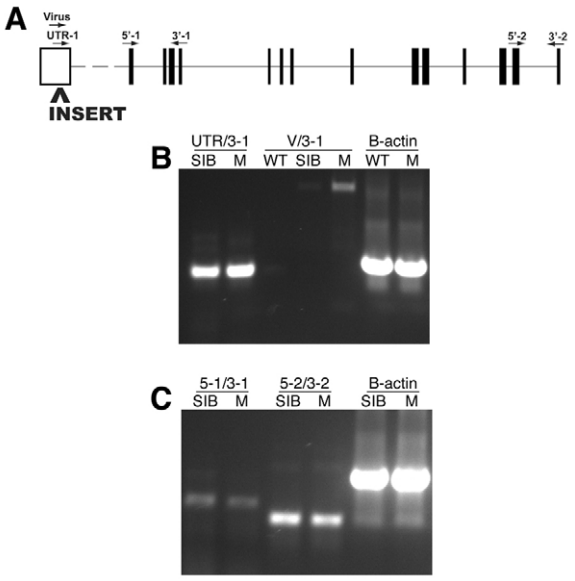

Fig. 4. Molecular analysis of the *gart*^{hi3526b} locus. (**A**) The approximate position of the proviral insertion and RT-PCR primers mapped onto a schematic of the mutated gene (www.ensembl.org/Danio_rerio/). The proviral insertion is located in the predicted 5′ UTR. Amplification of the region between the UTR and exon 4 (**B**, UTR/3-1), the region between exons 1 and 4 (**C**, 5-1/3-1), or the region between exons 13 and 14 (C, 5-2/3-2) all indicate that the overall levels of *gart* transcripts are unaffected in the homozygous mutant embryos. Amplification from the 3′ end of the proviral insert to exon 4 (B, V/3-1) in homozygous *gart* mutants indicates that a portion of the proviral insert is transcribed and retained in the resulting mRNA. WT, wild-type AB; SIB, wild-type sibling mixture (+/+ and +/–); M, homozygous mutant.

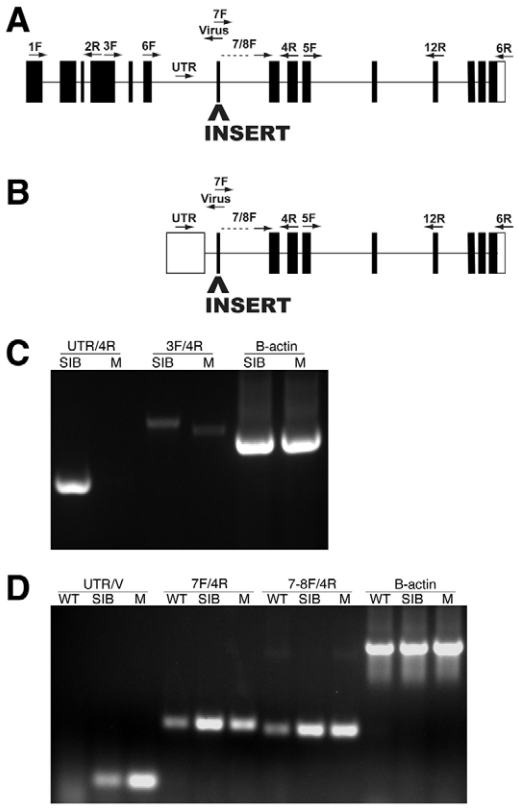

Fig. 5. Molecular analysis of the *paics*^{hi2688} locus. (**A**,**B**) The approximate position of the proviral insertion and RT-PCR primers mapped onto a schematic of the mutated gene (www.ensembl.org/Danio_rerio/). (A) *paics*^{LONG} is encoded by at least 15 exons, and all of the conserved enzymatic domains of the Paics protein are found in the sequence encoded by exons 7-15. The proviral insert in *paics* mutants is located in exon 7 of *paics*^{LONG}. (B) *paics*^{SHORT} is composed of the latter nine exons of *paics*^{LONG}, in addition to a tenth noncoding first exon. The proviral insert in *paics* mutants is located in exon 2 of *paics*^{SHORT}. (**C**) RT-PCR using primer sets that amplify the region between exons 4 and 9 of *paics*^{LONG} (3F/4R), and exons 1 and 4 of *paics*^{SHORT} (UTR/4R) indicates that both transcripts are expressed in wild-type embryos. Amplification of the region surrounding the site of proviral insertion (3F/4R) in *paics*^{LONG} indicates that the proviral insert leads to an alteration in mRNA splicing in the *paics*^{LONG} transcript. (**D**) RT-PCR using primer sets that assay for the presence of the proviral insert in *paics*^{SHORT} (UTR/V) indicates that the viral insert is present in *paics*^{SHORT} transcripts. RT-PCR amplification using *paics*^{SHORT}-specific exon 2 primers located downstream of the site of proviral insertion (7F/4R and 7-8F/4R) indicates that the virus sequence in *paics*^{SHORT} does not lead to detectable changes in transcript levels. WT, wild-type AB; SIB, wild-type sibling mixture (+/+ and +/–); M, homozygous mutant.

mapped onto a schematic of the mutated gene. RT-PCR was performed on total RNA samples isolated from 3 dpf wild-type AB, wild-type/heterozygous siblings and/or homozygous mutant embryos from each line, and transcript levels were assayed using primer sets flanking and/or downstream of the proviral insert. In *gart*^{hi3526b}, the proviral insertion is located in the predicted 5′ UTR, which is located roughly 5 kb from the predicted first coding exon (Fig. 4A). Amplification of the regions between the UTR and exon 4 (Fig. 4B), exons 1 and 4, or exons 13 and 14 (Fig. 4C) all indicated that the overall levels of *gart* were unaffected in the homozygous mutant embryos. However, amplification of the region spanning the 3′ end of the proviral insert and exon 4 revealed that in homozygous mutants, a portion of the proviral insert is transcribed and retained in the resulting mRNA (Fig. 4B), probably impairing translation and synthesis of Gart. Polyclonal antiserum derived against human GART did not recognize the zebrafish protein, so we were unable to confirm this experimentally.

Analysis of *paics* revealed the presence of at least two different transcripts in wild-type embryos (Fig. 5A,B), the first of which, *paics*^{LONG}, is encoded by at least 15 exons (Fig. 5A). All of the sequences encoding the conserved enzymatic domains of Paics are found in exons 7-15 of *paics*^{LONG}, and exon 7 contains a putative translational start site that would be predicted to generate a full-length Paics protein similar in size to the human ortholog. The second *paics* transcript, *paics*^{SHORT} (Fig. 5B), is composed of the latter nine exons of *paics*^{LONG}, in addition to a tenth noncoding first exon. The putative translational start site for *paics*^{SHORT} is located in exon 2. RT-PCR using primer sets that amplify the region between exon 4 and 9 of *paics*^{LONG} (primers 3F/4R in Fig. 5), and exon 1 and 4 of *paics*^{SHORT} (UTR/4R) indicates that both *paics* transcripts are expressed in wild-type embryos (Fig. 5C). Moreover, sequencing of these PCR products confirms this predicted intron/exon organization (data not shown).

The proviral insert in *paics*^{hi2688} mutants is located in exon 7 of *paics*^{LONG} and exon 2 of *paics*^{SHORT}. RT-PCR using primer sets that assay for the presence of the proviral insert in each of the transcripts (UTR/V) revealed that the viral insert is spliced into *paics*^{SHORT} (Fig. 5D) but not *paics*^{LONG} (data not shown). Conversely, using a primer

set that amplifies the region surrounding the site of proviral insertion (3F/4R) in *paics*^{LONG}, the proviral insert leads to an alteration in mRNA splicing whereby exon 7 is removed from *paics*^{LONG} (Fig. 5C), a result confirmed by DNA sequencing (data not shown). The finding that exon 7 is absent from *paics*^{LONG} enabled the utilization of primer sets within the corresponding exon 2 of *paics*^{SHORT}, but downstream of the proviral insertion (7F/4R and 7-8F/4R), to demonstrate that the presence of viral DNA in *paics*^{SHORT} does not lead to detectable changes in transcript levels of this splice form (Fig. 5D). We have not determined how much viral sequence is maintained in *paics*^{SHORT}; however, RT-PCR utilizing a primer set that amplifies exon 1 to exon 4 of *paics*^{SHORT} was not successful in homozygous mutant samples, even when PCR extension times were increased to over four minutes, suggesting that much of the virus is retained in the transcript (Fig. 5C). These data indicate that the proviral insertion disrupts *paics*^{LONG} by causing exon 7 to be spliced out, either preventing translation of *paics*^{LONG}, if exon 7 contains the translational start site, or resulting in a translational frameshift, if exon 7 is located within the endogenous Paics^{LONG} protein. For *paics*^{SHORT}, data indicate that the proviral insertion does not affect transcript levels; rather, it probably prevents translation of *paics*^{SHORT}. Polyclonal antiserum derived against human PAICS did not recognize the zebrafish protein, so we were unable to confirm this experimentally.

To begin to understand the developmental defects in *gart* and *paics* mutants, we first wanted to determine their expression profiles (Fig. 6A,B). Maternal *gart* expression was detected by RT-PCR at the 2-cell stage and maintained expression was detected at 1, 3 and 6 dpf (Fig. 6A). To assay *paics* expression, and to differentiate between the two *paics* splice forms, we utilized a primer set that amplifies the region between exons 6 and 12 (6F/12R), which will only amplify *paics*^{LONG}, and a primer set that amplifies the region from the noncoding exon 1 (intron 6 in *paics*^{LONG}) to exon 7 (UTR/12R) that will only amplify *paics*^{SHORT}. Interestingly, only *paics*^{SHORT} was provided maternally, whereas maintained zygotic expression of both splice forms was detected at 1, 3 and 6 dpf (Fig. 6B). *gart* and *paics* are highly expressed within the eye, central nervous system and pigment cells throughout development (Thisse and Thisse, 2004) (data not shown).

Maternally provided *gart* and *paics* is required for normal embryonic development

Given the maternal expression of both *gart* and *paics*, we reasoned that more severe developmental phenotypes were probably masked in zygotic mutants due to the presence of maternal transcripts. To test this hypothesis, we crossed homozygous *gart* and *paics* females to homozygous or heterozygous males to generate maternal-zygotic mutants (*gart*^{MZ} and *paics*^{MZ}), and maternal-effect mutants (*gart*^{ME} and *paics*^{ME}), which lacked both maternal mRNA and protein and a functional maternal copy of each gene. These latter mutants enabled us to assay whether the zygotic paternal genome alone could direct normal embryonic development. *gart*^{ME} mutants were drastically delayed in development when compared with wild-type embryos derived from heterozygous incrosses (Fig. 6C,D). Most *gart*^{ME} mutants lived for ~36-48 hpf and then began to degenerate, dying by 3 dpf. Despite this high degree of lethality, we were able to rear a small number of *gart*^{ME} mutants to adulthood. These fish were runted over their first 2-3 months but eventually grew to near wild-type size, showing normal pigmentation and no overt defects (data

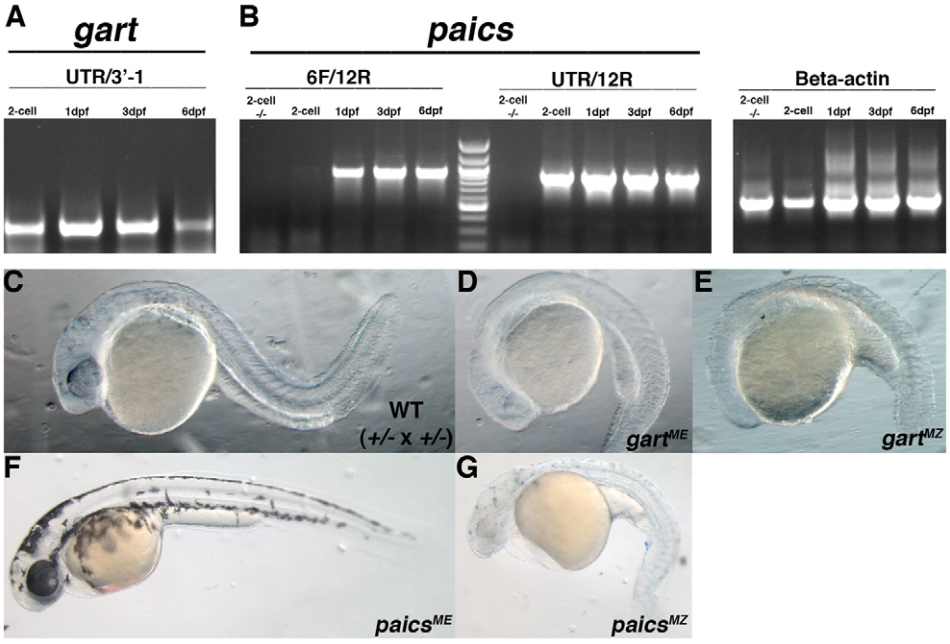

Fig. 6. *gart* and *paics* are maternally provided and limit the severity of phenotypes in zygotic mutants. (**A**) RT-PCR analysis of *gart* indicates maternal expression at the 2-cell stage and sustained zygotic expression at 1, 3 and 6 dpf. (**B**) RT-PCR analysis of *paics*^{LONG} (6F/12R) and *paics*^{SHORT} (UTR/12R) at the 2-cell stage and 1, 3 and 6 dpf. Only *paics*^{SHORT} is provided maternally, whereas maintained zygotic expression of both splice forms was detected at 1, 3 and 6 dpf. *beta actin* was used as a control. (**C**) Wild-type sibling derived from a *gart*$^{+/-}$ × *gart*$^{+/-}$ cross at 28 hpf. (**D**) *gart* maternal-effect mutants (*gart*^{ME}) at 28 hpf are drastically delayed in development when compared with wild-type embryos derived from heterozygous incrosses. (**E**) *gart* maternal-zygotic (*gart*^{MZ}) mutants at 28 hpf have arrested in development and display severe defects in anterior development. (**F**) *paics* maternal-effect mutants (*paics*^{ME}) at 52 hpf have pigmentation defects and microphthalmia but are relatively normal otherwise. (**G**) *paics* maternal-zygotic (*paics*^{MZ}) mutant at 52 hpf. *paics*^{MZ} mutants are small, nearly albino and possess cardiac edemas and widespread CNS degeneration.

not shown). All *gart*^{MZ} mutants arrested in development at ~16-18 hpf, displaying severe defects in anterior development (Fig. 6E). Surprisingly, *paics*^{ME} mutants developed relatively normally throughout the first 2-3 days of embryonic development (Fig. 6F), but after this point they began to degenerate and most died 5-7 dpf. *paics*^{ME} mutants resembled mutants derived from heterozygous mothers, indicating that zygotic expression of the paternal copy of *paics* was unable to rescue pigment formation or eye growth. Beyond these defects however, no additional phenotypes were observed prior to the onset of degeneration in *paics*^{ME} mutants. Like *gart*^{ME} mutants, a small number of *paics*^{ME} fish were viable and although they were runted during the first few months, as adults they were also normal (data not shown). *paics*^{MZ} mutants survived longer than *gart*^{MZ} mutants, developing to ~60-72 hpf before dying. *paics*^{MZ} mutants were small, nearly albino and possessed cardiac edemas and widespread CNS degeneration (Fig. 6G). RT-PCR using total RNA isolated from 2-cell-stage *paics*^{MZ} embryos revealed that, as expected, *paics*^{MZ} mutants lacked expression of maternally provided *paics*^{SHORT} transcripts (Fig. 6B).

Pigmentation defects in *gart* and *paics* mutants probably arise from defects in pigment synthesis

We next wanted to determine the underlying cellular mechanisms of the pigmentation phenotypes in *gart* and *paics* mutants. Two possible models to explain these defects are: (1) pigment cells are not properly specified or are not able to properly migrate and generate the larval pigment pattern; or (2) pigment cell specification and migration are normal, but these cells are impaired in their biochemical ability to synthesize pigments. Quantification of melanin levels in *gart* and *paics* mutants supports the latter of these models (see Fig. S1 in the supplementary material). Histological and TEM imaging of the pigmented iris and RPE enabled a rapid analysis of each pigment cell type (Fig. 7A,C). Additionally, examination of the posterior of the eye enabled a secondary analysis of melanosomes in the RPE and of iridophores within the sclera (Fig. 7B). In wild-type eyes, a dense layer of melanosome-containing RPE is obvious and within the iris one can observe numerous round pterinosomes and several iridosomes, which appear reflective due to the highly ordered guanine stacks (Fig. 7A). TEM analysis highlights the presence of these organelles: melanosomes in the RPE, and pterinosomes and guanine stacks in iridosomes within the iris (Fig. 7C). At the posterior of the eye, the RPE contains melanosomes and the sclera contains interspersed iridosomes (Fig. 7B). *gart* and *paics* mutants possess each of these pigment cell types, supporting the hypothesis that their specification and differentiation are unaffected in the mutants. However, the number of pigment-containing pterinosomes and iridosomes appears to be reduced in the iris (Fig. 7D,F,G,I) and to a lesser extent in the RPE and sclera (Fig. 7E,H) of the mutants,

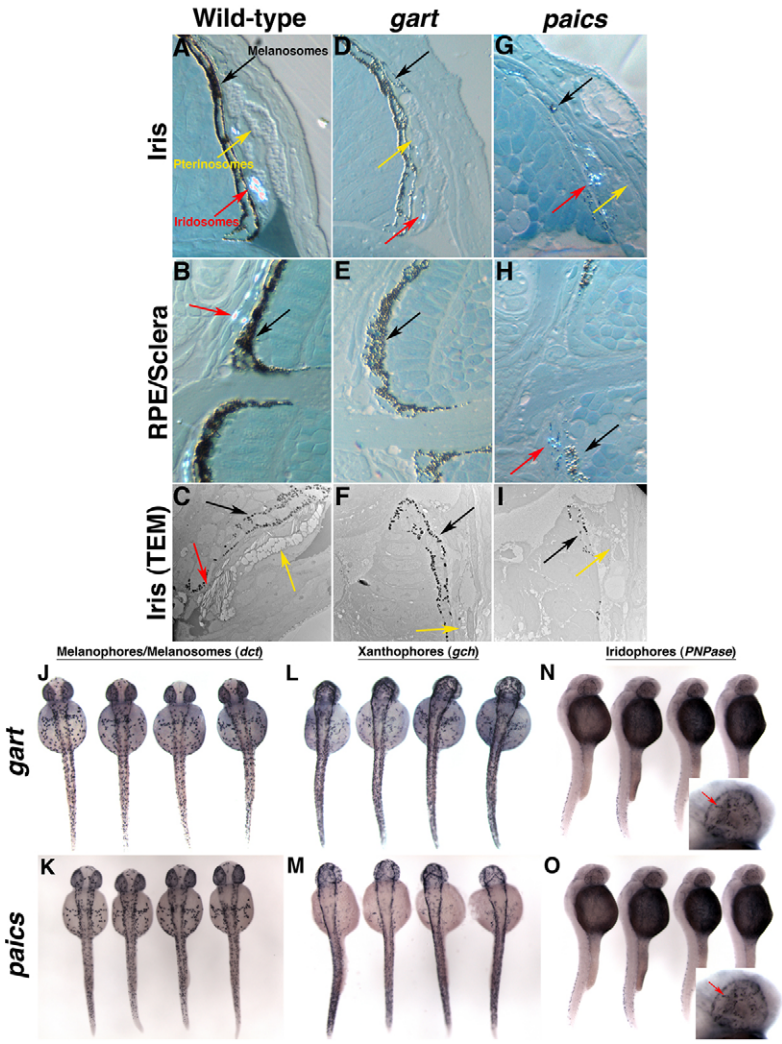

Fig. 7. Pigment-containing organelles and cell types are normal in *gart* and *paics* mutants. (**A-I**) High magnification images of transverse histological sections through wild-type (A,B), *gart* (D,E) and *paics* (G,H) eyes indicating the presence of melanosomes (black arrow), pterinosomes (yellow arrow) and iridosomes (red arrow) in the pigmented iris (A,D,G) and of melanosomes and iridosomes in the RPE and sclera (B,E,H). (C,F,I) TEM images of the iris of wild type (C), *gart* (F) and *paics* (I). (**J-O**) In situ hybridization for pigment cell types in representative embryos derived from *gart* (J,L,N) and *paics* (K,M,O) heterozygous incrosses. (J,K) *dct* marks melanocytes and melanosomes in the RPE. (L,M) *gch* marks xanthophores. (N,O) *PNPase* marks iridophores. Inset in N and O, high magnification view of iridophores in the eye (arrows). No differences in the number or distribution of pigment cells were observed between wild-type and mutant embryos (not shown).

suggesting that in the absence of sufficient pigment, the formation or integrity of these pigment-containing organelles might be compromised.

To further analyze pigmentation defects in *gart* and *paics* mutants, we utilized in situ hybridization markers for pigment cell types to determine if their overall number or distribution was compromised. *dopachrome tautomerase* (*dct*) encodes a protein that converts dopachrome to 5,6-dihydroxyindole-2-carboxylic acid (DHICA) and 5,6-dihydroxyindole (DHI) in melanosomes (Fig. 11). Using *dct* as a marker for melanosomes, no obvious differences in the number or distribution of melanocytes within the dermis, or in the intensity of expression in the RPE, were noted in *gart* or *paics* mutants (Fig. 7J,K). Similarly, using *GTP cyclohydrolase I* (*gch*, *gch2* – ZFIN), which encodes a protein that converts GTP to 6-pyruvoyl-H_4 pterin synthase, as a marker for xanthophores (Fig. 7L,M), and *purine nucleotide phosphorylase* (*PNPase*, *xdh* – ZFIN), which encodes a protein that converts inosine to hypoxanthine, as a marker for iridophores (Fig. 7N,O), revealed no obvious differences in the number or distribution of these cell types in the mutants.

gart and *paics* function are required for eye growth

ATP levels influence cell proliferation in a number of contexts, and recent studies have highlighted a crucial role for RPE-released ATP in regulating retinoblast proliferation in the developing eye (Martins and Pearson, 2008; Pearson et al., 2002; Pearson et al., 2005). The findings that the proteins encoded by *gart* and *paics* provide IMP, the precursor for ATP (Fig. 1), and *gart* and *paics* mutants are microphthalmic (Figs 2,3), suggested that these proteins might play a role in regulating eye growth. We envisioned two possible mechanisms that could underlie the microphthalmia in the mutants: (1) defects in retinoblast proliferation, whereby the cell cycle in retinoblasts is prolonged or cell cycle exit is compromised, could lead to a smaller eye; and/or (2) increases in apoptosis could lead to a smaller eye. To test the first of these hypotheses we utilized BrdU incorporation assays to compare the percentage and location of proliferative cells between wild-type and mutant eyes (Fig. 8). BrdU incorporation from 48 to 50 hpf indicated that 20.3% of cells in the wild-type retina were in S phase (Fig. 8H), and most were located at the retinal periphery (Fig. 8A). By comparison, 40.9% of cells in the *paics* retina were in S phase (Fig. 8H), and these cells were ectopically located throughout the central retina (Fig. 8B). BrdU incorporation from 54 to 56 hpf indicated that 13.9% of cells in the wild-type retina were in S phase (Fig. 8H), and nearly all of these were located at the ciliary marginal zones (CMZs; Fig. 8C). In the *gart* retina, 25.5% of cells were in S phase (Fig. 8H) and, like *paics*, they were ectopically located within the central retina (Fig. 8D). BrdU incorporation from 96 to 98 hpf indicated that 2.9% of cells in the wild-type retina were in S phase (Fig. 8H), and again, all of these were located at the retinal periphery (Fig. 8E). By comparison, 5.5% of the *paics* retina and 6.6% of the *gart* retina was BrdU-positive (Fig. 8H); however, all of these S-phase cells were confined to the retinal periphery (Fig. 8F,G).

Histological analysis did not identify pyknotic nuclei in *gart* and *paics* mutant eyes at the time at which microphthalmia was first identifiable (Fig. 3A-D). To further test the latter hypothesis for microphthalmia, we utilized TUNEL staining to identify apoptotic nuclei. As reported by others (Cole and Ross, 2001; Biehlmaier et al., 2001), apoptotic nuclei in the wild-type retina were rare (Fig. 8I,K). No differences in the number of TUNEL$^+$ cells were detected between wild-type siblings and *paics* mutants at 48 hpf (Fig. 8I,J) or *gart* mutants at 54 hpf (Fig. 8K,L), nor were differences detected at later time points (data not shown). Thus, apoptosis is not likely to contribute to the microphthalmia in *gart* and *paics* mutants. An absence of increased levels of cell death, combined with an increase in the proportion of the mutant retina that is BrdU$^+$, supports the hypothesis that defects in cell cycle progression lead to microphthalmia in *gart* and *paics* mutants.

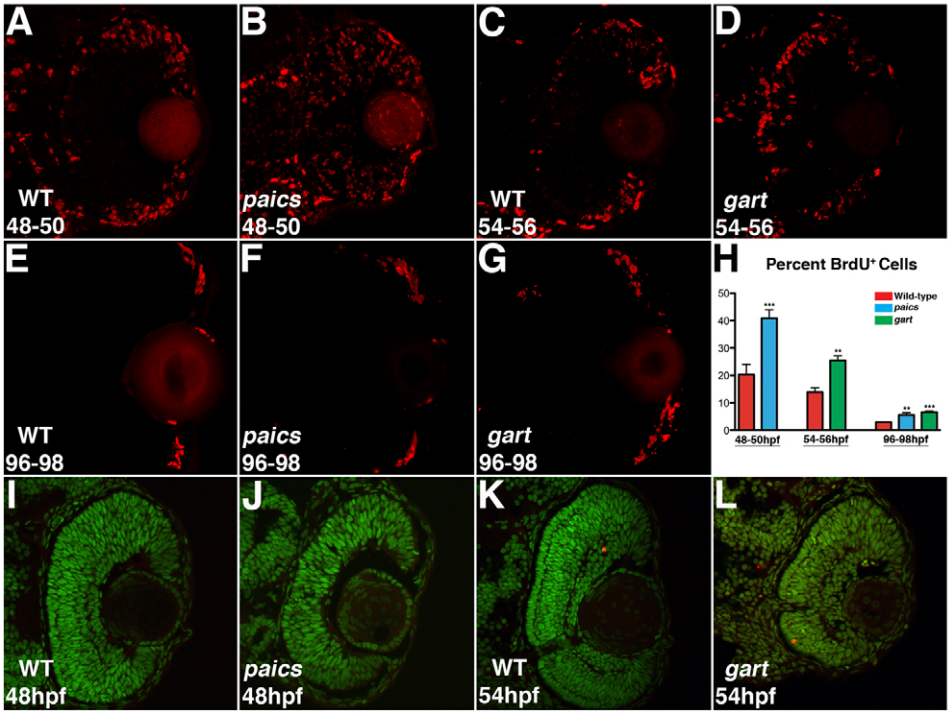

Fig. 8. Cell proliferation and apoptosis in *gart* and *paics* mutants. (**A**,**C**) BrdU exposures 48-50 hpf and 54-56 hpf indicate that in the wild-type eye most proliferative cells are located at the retinal periphery. (**B**) In *paics* and (**D**) *gart* mutants, BrdU$^+$ cells are located throughout the central retina. (**E-G**) BrdU exposures 96-98 hpf localized proliferative cells in the wild-type and both *paics* and *gart* mutant retinas to the retinal periphery. (**H**) Quantifying the percentage of BrdU$^+$ cells in each retina identified significant increases in the *paics* and *gart* mutants at each time point (** P<0.05, *** P<0.001). (**I-L**) TUNEL labeling to identify apoptotic nuclei. No increases in apoptosis over wild-type levels were observed in *paics* mutants at 48 hpf (I,J) or *gart* mutants at 54 hpf (K,L).

IMP feeds into an 'ATP pathway' required for retinoblast proliferation and a 'GTP pathway' required for pigmentation

IMP serves as a precursor for both ATP and GTP biosynthesis (Fig. 11). ATP can modulate retinoblast proliferation and cell cycle duration within the developing vertebrate eye (Pearson et al., 2002; Pearson et al., 2005), whereas components downstream of GTP are involved in zebrafish pigmentation (Le Guyader et al., 2005; Ziegler, 2003), suggesting independent functions for the two purines during development. Since Gart and Paics function in IMP synthesis upstream of the ATP and GTP synthesis pathways, it is not surprising that *gart* and *paics* mutants display both microphthalmia and pigmentation phenotypes. We wanted to test this model predicting that the ATP and GTP pathways were separable into distinct developmental roles, and we hypothesized that if one perturbed only the ATP synthesis pathway, microphthalmia with normal pigmentation should result. Conversely, if one perturbed only the GTP synthesis pathway, pigmentation defects should result, but eye size would be unaffected.

To test the hypothesis that the ATP pathway is involved in regulating eye growth, we designed a morpholino antisense oligo targeting the intron 1/exon 2 splice junction of *adenylosuccinate synthase* (*adss*; adss-MO; Fig. 9C). *adss* encodes the protein that catalyzes the first reaction in the ATP pathway, converting IMP to adenylosuccinate (Fig. 11). Injection of 3.33 ng of adss-MO resulted in an absence of *adss* transcripts in *adss* morphants', probably through nonsense-mediated mRNA decay (see Fig. S4A in the supplementary material). As predicted, *adss* morphants were microphthalmic, with eye size reduced by almost 30% (Fig. 9D,E; Table 2). Importantly, however, pigmentation was unaffected; xanthophore, iridophore and melanophore/RPE pigmentation all appeared similar to that observed in control MO-injected siblings. Additionally, an insertional mutation affecting *adss* has been reported and, phenotypically, *adss*^{hi3081} mutants have microphthalmia but normal pigmentation (Amsterdam et al., 2004) (data not shown).

To test the hypothesis that GTP feeds into a pathway required for pigmentation and not eye growth, we utilized a morpholino targeting the exon 2/intron 2 splice junction of *GMP synthase* (*gmps*; gmps-MO; Fig. 9F), which encodes the enzyme that converts XMP to GMP (Fig. 11). Injection of 3.9 ng of gmps-MO disrupted splicing of exon 2 of *gmps*, as verified by RT-PCR (see Fig. S4B in the supplementary material) and DNA sequencing (see Fig. S4C in the supplementary material). All *gmps* morphants possessed obvious pigmentation defects that resembled zygotic *gart* and *paics* mutants. Melanin pigmentation was reduced at 36 hpf (data not shown), and there was a near absence of xanthophore and iridophore pigmentation at 3 dpf (Fig. 9G,H). Eye size was largely unaffected, although the eyes of *gmps* morphants were 4% smaller than those in control-injected embryos (Table 2).

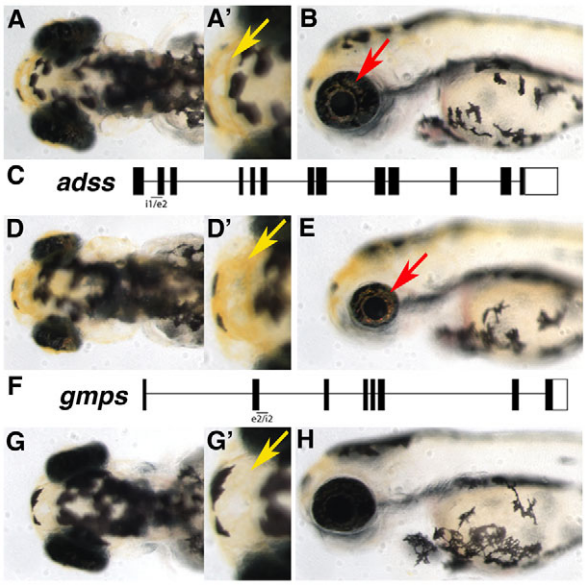

Fig. 9. Requirement for *adss* in eye growth and *gmps* in pigmentation downstream of *gart* and *paics*. (**A-B**) Dorsal (A,A′) and lateral (B) images of control MO-injected embryos at 3 dpf. Xanthophores (yellow arrow) and iridophores (red arrow) are highlighted. (**C**) The *adss* locus and approximate position of the morpholino target site. (**D-E**) *adss* morphants are microphthalmic but have normal pigmentation. (**F**) The *gmps* locus and approximate position of the morpholino target site. (**G-H**) *gmps* morphants have nearly normal sized eyes but lack most xanthophore- and iridophore-derived pigmentation. Xanthophores can be observed (G′) but are markedly lighter than those in control-injected embryos (A′).

ATP pathway function is required for S-phase progression in proliferative retinoblasts

We next wanted to determine the cellular mechanism through which the ATP pathway regulated eye growth. Like *gart* and *paics* mutants, *adss* morphants possessed a significantly higher proportion of BrdU^{+} cells in their retinas when compared with control MO-injected embryos (Fig. 10A), and many of these were ectopically located within the central retina (data not shown). These results suggest at least two possible roles for the ATP pathway in regulating the cell cycle in retinoblasts: it could be required for normal S-phase progression; and/or it could be required for S-phase exit and G2/M progression. To test these models, we utilized flow cytometry to quantify DNA content and compare the proportions of retinal cells in each phase of the cell cycle between control MO-injected and *adss* morphant retinas. Quantification at 48 hpf and 72 hpf revealed significant changes in the proportion of cells in the G1 and S phases of the cell cycle in the *adss* morphant retina, when compared with controls (Fig. 10B,C). At both times, the proportion of cells in the S phase was increased in the *adss* morphant retina, whereas the proportion of cells in the G1 phase was decreased. The proportion of cells in the G2/M phases was also decreased in the *adss* morphant retina, but these differences were not statistically significant at either time point (P<0.05). *cyclin d1* (*ccnd1*) serves as a marker of the G1/S transition, and, generally, of proliferative cells in the retina (Levine and Green, 2004). In control MO-injected embryos, *ccnd1* is localized to the zones of proliferative cells at the retinal periphery at 48 hpf (Fig. 10D). In *adss* morphants, *ccnd1* remained expressed within the central retina (Fig. 10D), indicating that these cells had not exited the cell cycle. *cyclin b1* (*ccnb1*), a marker of the G2/M transition (Nasmyth, 1996), was distributed normally in *adss* morphants, however (Fig. 10D). An expansion of *ccnd1* into the central retina of *adss* morphants correlates with the increased number of BrdU^{+} cells in the central retina of *gart* and *paics* mutants, and *adss* morphants, and it correlates with the increased proportion of S-phase cells found in the *adss* morphant retina. When combined, these data support a model in which the ATP pathway is required in retinoblasts for their timely progression through S phase. When the pathway is impaired, S phase is prolonged, the rate of cell division decreases and microphthalmia results.

Table 2. Eye size measurements of morphant embryos at 3 dpf

Morpholino	A/P axis	D/V axis	N/T axis
Control	259.6±3.51	218.4±5.18	165.4±3.97
adss	183.8±11.2 P=4.1×10^{-5}	155.2±6.8 P=3.7×10^{-7}	118.6±8.1 P=3.0×10^{-5}
gmps	248.8±6.69 P=0.0184	209.2±5.26 P=0.0237	158.8±7.73 P=0.1405

Measurements (in μm) were made along the anterior/posterior (A/P), dorsal/ventral (D/V) and nasal/temporal (N/T) axes of ten morpholino-injected embryos and averaged. P values are indicated.

DISCUSSION

Using zebrafish mutations and/or morpholino-induced loss of function in *gart*, *paics*, *adss* and *gmps*, our results support a model in which de novo purine synthesis is required for two diverse developmental functions: an ATP pathway mediates eye growth by regulating retinoblast proliferation and cell cycle progression, and a GTP pathway mediates embryonic pigmentation, probably serving as a precursor for the biosynthesis of each of the pigment molecules (Fig. 11). Zygotic loss of function for *gart* and *paics* affects de novo purine biosynthesis upstream of the bifurcation of the ATP and GTP pathways, and therefore *gart* and *paics* mutants show defects in both eye growth and pigmentation. *adss* mutants and morphants are only affected in the ATP pathway, and this results in eye growth defects resembling those in *paics* and *gart*, but with normal pigmentation. Conversely, *gmps* morphants are only affected in the GTP pathway and this results in *paics* and *gart*-like pigmentation defects but relatively normal eye size. Our data do not exclude the possibility that the GTP pathway also contributes to eye growth because eye size was mildly smaller in *gmps* morphants; however, this contribution is likely to be far less significant than that of the ATP portion given the substantial decrease in eye size observed in *adss* mutants and morphants. Finally, we demonstrate a crucial role for maternal *gart* and *paics* function as both maternal-zygotic and maternal-effect mutants display more severe developmental defects than their zygotic counterparts. These results highlight a crucial role for de novo purine synthesis during vertebrate development and they further subdivide these developmental roles into those that depend on ATP- or GTP-specific pathways.

Our results, when coupled with those from several previous reports, provide possible mechanistic insights into the phenotypes observed in *gart*, *paics*, *adss* and *gmps* mutants and morphants and into how de novo purine biosynthesis mediates such diverse developmental functions. With regard to retinoblast proliferation and cell cycle progression, it has been demonstrated that ATP, released from the RPE, can nonautonomously modulate the rate of the retinoblast cell cycle and thereby regulate overall rates of eye growth (Martins and Pearson, 2008; Pearson et al., 2002; Pearson et al., 2005). Using chicken retinal explants and pharmacological manipulations, ATP was shown to mechanistically act by modulating the rate of mitosis (Pearson et al., 2002) and/or the rate of DNA synthesis (Sugioka et al., 1999; Pearson et al., 2005). Given the key enzymatic roles that the proteins encoded by the *gart*, *paics* and *adss* loci play in the biosynthesis of ATP, the most parsimonious explanation for the cellular mechanism underlying the microphthalmia observed in *gart*, *paics* and *adss* zebrafish mutants and/or morphants is that, in the absence of sufficient ATP, DNA synthesis during S phase is delayed. This leads to a net lengthening of the cell cycle in each retinoblast, as well as a higher overall proportion of retinoblasts within the developing eye remaining in S phase. Over time, each round of cell division takes longer, leading to fewer total cells in the retina and, thus, to microphthalmia. Homozygous *gart* and *paics* mutants eventually recover and, as adults, eye size is normal, which is likely to reflect the activity of the nucleotide salvage pathway.

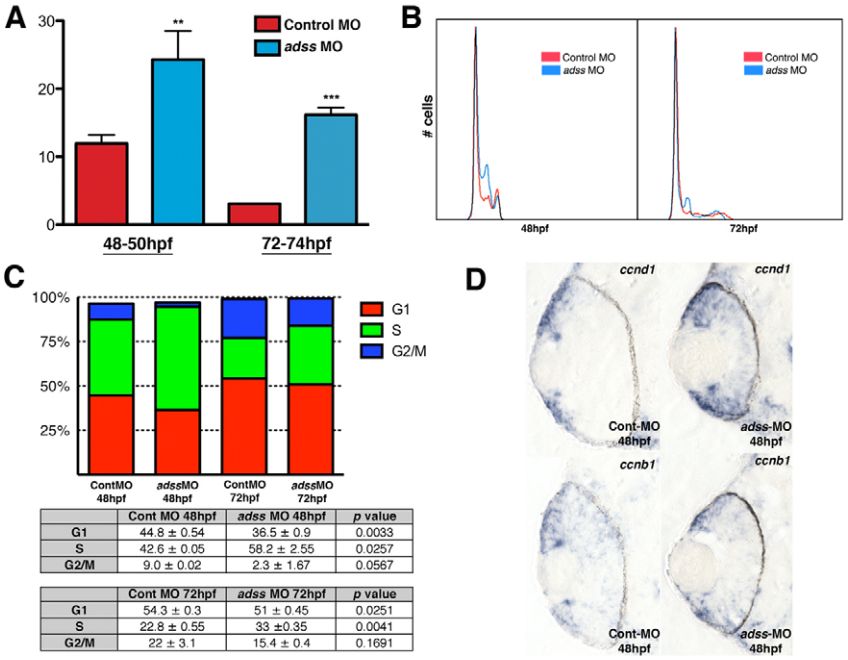

	Cont MO 48hpf	*adss* MO 48hpf	*p* value
G1	44.8 ± 0.54	36.5 ± 0.9	0.0033
S	42.6 ± 0.05	58.2 ± 2.55	0.0257
G2/M	9.0 ± 0.02	2.3 ± 1.67	0.0567

	Cont MO 72hpf	*adss* MO 72hpf	*p* value
G1	54.3 ± 0.3	51 ± 0.45	0.0251
S	22.8 ± 0.55	33 ±0.35	0.0041
G2/M	22 ± 3.1	15.4 ± 0.4	0.1691

Fig. 10. The ATP pathway is required for S-phase progression. (**A**) BrdU exposures 48-50 hpf and 72-74 hpf indicate a higher proportion of S-phase cells (*y*-axis) in *adss* morphants (** P<0.05, *** P<0.005). (**B**) DNA content analysis plots from flow cytometry at 48 hpf and 72 hpf. (**C**) Graphical and tabular data for percentage of cells in G1, S or G2/M, as determined by flow cytometry. *adss* morphants possess elevated percentages of cells in S phase and decreased percentages in G1. (**D**) *ccnd1* expression is expanded into the central retina of *adss* morphants when compared with control MO-injected embryos. *ccnb1* distribution is normal.

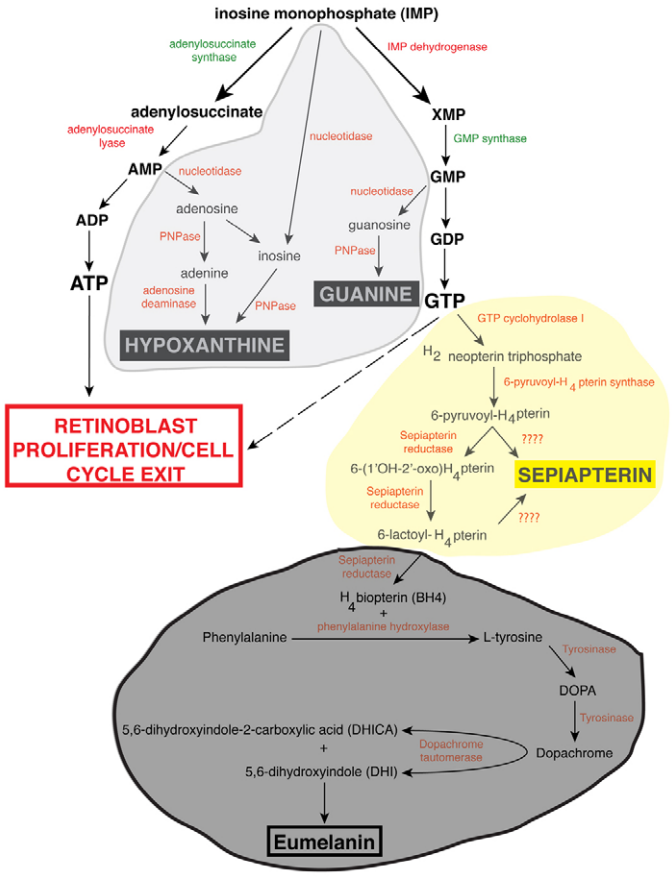

Fig. 11. Model for ATP- and GTP-specific developmental pathways during zebrafish embryogenesis. IMP feeds into the ATP and GTP pathways. The ATP pathway facilitates retinoblast proliferation and S-phase exit. The GTP pathway facilitates pigment synthesis: guanine in iridophores, sepiapterin in xanthophores and eumelanin in melanosomes/melanocytes (Le Guyader et al., 2005; Ziegler, 2003). Iridophore pathways are shaded light gray, xanthophore pathways are shaded yellow and melanophore/RPE pathways are shaded dark gray. Enzymes are in red, except those targeted by morpholinos, which are green.

With respect to the pigmentation defects in *gart* and *paics* mutants and *gmps* morphants, our results support a model whereby Gart- and Paics-dependent IMP formation feeds into a Gmps-dependent GTP pathway that impinges on the synthesis of the three pigment types (Fig. 11). GTP is thought to serve as the precursor for synthesis of each of these pigment molecules (Ziegler, 2003), and in the absence of sufficient IMP levels (*gart* and *paics*) or the ability to convert XMP to GMP (*gmps* morphants) pigment molecules are absent or deficient. The finding that pigmentation recovers in homozygous adult *gart* and *paics* mutants again probably reflects the activity of the salvage pathway.

Interestingly, developmental phenotypes in *gart* and *paics* mutants are different than those resulting from deficiencies in de novo pyrimidine biosynthesis (Link et al., 2001; Willer et al., 2005). In the pyrimidine biosynthesis mutant *perplexed*, the gene encoding Cad, an enzyme that catalyzes the first three steps of de novo pyrimidine synthesis, is disrupted (Willer et al., 2005). *perplexed* mutants have defects in both proliferation and neuronal differentiation within the retina, and they possess defects in jaw and pectoral fin formation. Pigmentation in these mutants is normal, however. Additionally, de novo pyrimidine mutants in *Drosophila* often possess defects in wing formation (Rawls and Fristrom, 1975; Falk, 1976), whereas mutants in de novo purine biosynthesis have defects in eye color (Tiong et al., 1989). These studies, when combined with our results, support a model in which de novo purine biosynthesis and de novo pyrimidine biosynthesis play important but tissue-specific roles during animal development.

Two human congenital disorders have been described that affect the de novo purine synthesis pathway. The first, adenylosuccinate lyase deficiency, disrupts *adenylosuccinate lyase* (*ADSL*), whose protein product catalyzes two stages of de novo purine synthesis: (1) the eighth step in IMP synthesis (Fig. 1); and (2) the conversion of adenylosuccinate to AMP in the ATP pathway (Fig. 11) (Marie et al., 1999; Spiegel et al., 2006; Stone et al., 1992). Patients with *ADSL* mutations have severe mental retardation, epilepsy and autistic features, although no ocular phenotypes have been reported. The second disorder, AICA-ribosiduria, results from a deficiency in *ATIC*, whose protein product catalyzes the ninth and tenth reactions of IMP synthesis (Fig. 1). The only reported patient with this disorder had dysmorphic features of the face and body, mental retardation, epilepsy and congenital blindness (Marie et al., 2004). The molecular underpinnings of these disorders are not well understood, however, it has been demonstrated that the substrates for each enzyme accumulate in afflicted patients, suggesting that these intermediates might be deleterious for neuronal development and function. Zebrafish models of de novo purine synthesis deficiencies might thus be useful in elucidating how defects in this pathway can lead to defects in human embryonic development and CNS function.

Acknowledgements
We thank Brian Link for helpful discussions and for providing *adssl*^{hi3081} embryos; Richard Salinas, Cindy Yang, Maria Tavares and Fernando Casares for advice on FACS analysis; and Jonathan Richman for technical assistance. This work was funded by grants from the Karl Kirchgessner Foundation, NSF (IOS-0745782) and NIH (RO1-EY18005) to J.M.G., F31-EY019239 to R.A.U., and by undergraduate fellowships to A.N. and L.Y. *gart*^{hi3526b} embryos, cDNAs and antisera were obtained from ZIRC, supported by NIH-NCRR grant P40 RR012546. Deposited in PMC for release after 12 months.

Supplementary material
Supplementary material for this article is available at
http://dev.biologists.org/cgi/content/full/136/15/2601/DC1

References
Amsterdam, A., Nissen, R. M., Sun, Z., Swindell, E. C., Farrington, S. and Hopkins, N. (2004). Identification of 315 genes essential for early zebrafish development. *Proc. Natl. Acad. Sci. USA* **101**, 12792-12797.
Bessa, J., Tavares, M. J., Santos, J., Kikuta, H., Laplante, M., Becker, T. S., Gomez-Skarmeta, J. and Casares, F. (2008). meis1 regulates cyclin D1 and c-myc expression and controls the proliferation of the multipotent cells in the early developing zebrafish eye. *Development* **135**, 799-803.
Biehlmaier, O., Neuhauss, S. C. and Kohler, K. (2001). Onset and time course of apoptosis in the developing zebrafish retina. *Cell Tissue Res.* **306**, 199-207.
Clark, D. V. (1994). Molecular and genetic analyses of Drosophila Prat, which encodes the first enzyme of de novo purine biosynthesis. *Genetics* **136**, 547-557.
Cole, L. K. and Ross, L. S. (2001). Apoptosis in the developing zebrafish embryo. *Dev. Biol.* **240**, 123-142.
Falk, D. R. (1976). Pyrimidine auxotropy and the complementation map of the rudimentary locus of Drosophila melanogaster. *Mol. Gen. Genetics* **148**, 1-8.
Golling, G., Amsterdam, A., Sun, Z., Antonelli, M., Maldonado, E., Chen, W., Burgess, S., Haldi, M., Artzt, K., Farrington, S. et al. (2002). Insertional mutagenesis in zebrafish rapidly identifies genes essential for early vertebrate development. *Nat. Genet.* **31**, 135-140.
Gross, J. M., Perkins, B. D., Amsterdam, A., Egana, A., Darland, T., Matsui, J. I., Sciascia, S., Hopkins, N. and Dowling, J. E. (2005). Identification of zebrafish insertional mutants with defects in visual system development and function. *Genetics* **170**, 245-261.
Henikoff, S., Keene, M. A., Sloan, J. S., Bleskan, J., Hards, R. and Patterson, D. (1986a). Multiple purine pathway enzyme activities are encoded at a single genetic locus in Drosophila. *Proc. Natl. Acad. Sci. USA* **83**, 720-724.

Henikoff, S., Nash, D., Hards, R., Bleskan, J., Woolford, J. F., Naguib, F. and Patterson, D. (1986b). Two Drosophila melanogaster mutations block successive steps of de novo purine synthesis. *Proc. Natl. Acad. Sci. USA* **83**, 3919-3923.
Johnstone, M. E., Nash, D. and Naguib, F. N. (1985). Three purine auxotrophic loci on the second chromosome of Drosophila melanogaster. *Biochem. Genet.* **23**, 539-555.
Jowett, T. and Lettice, L. (1994). Whole-mount in situ hybridizations on zebrafish embryos using a mixture of digoxigenin- and fluorescein-labelled probes. *Trends Genet.* **10**, 73-74.
Lee, J., Willer, J. R., Willer, G. B., Smith, K., Gregg, R. G. and Gross, J. M. (2008). Zebrafish blowout provides genetic evidence for Patched1-mediated negative regulation of Hedgehog signaling within the proximal optic vesicle of the vertebrate eye. *Dev. Biol.* **319**, 10-22.
Le Guyader, S., Maier, J. and Jesuthasan, S. (2005). Esrom, an ortholog of PAM (protein associated with c-myc), regulates pteridine synthesis in the zebrafish. *Dev. Biol.* **277**, 378-386.
Levine, E. M. and Green, E. S. (2004). Cell-intrinsic regulators of proliferation in vertebrate retinal progenitors. *Semin. Cell Dev. Biol*. **15**, 63-74.
Link, B. A., Kainz, P. M., Ryou, T. and Dowling, J. E. (2001). The perplexed and confused mutations affect distinct stages during the transition from proliferating to post-mitotic cells within the zebrafish retina. *Dev. Biol.* **236**, 436-453.
Long, H., Cameron, S., Yu, L. and Rao, Y. (2006). De novo GMP synthesis is required for axon guidance in Drosophila. *Genetics* **172**, 1633-1642.
Maldonado, E., Hernandez, F., Lozano, C., Castro, M. E. and Navarro, R. E. (2006). The zebrafish mutant vps18 as a model for vesicle-traffic related hypopigmentation diseases. *Pigment Cell Res.* **19**, 315-326.
Marie, S., Cuppens, H., Heuterspreute, M., Jaspers, M., Tola, E. Z., Gu, X. X., Legius, E., Vincent, M. F., Jaeken, J., Cassiman, J. J. et al. (1999). Mutation analysis in adenylosuccinate lyase deficiency: eight novel mutations in the re-evaluated full ADSL coding sequence. *Hum. Mutat.* **13**, 197-202.
Marie, S., Heron, B., Bitoun, P., Timmerman, T., Van Den Berghe, G. and Vincent, M. F. (2004). AICA-ribosiduria: a novel, neurologically devastating inborn error of purine biosynthesis caused by mutation of ATIC. *Am. J. Hum. Genet.* **74**, 1276-1281.
Martins, R. A. and Pearson, R. A. (2008). Control of cell proliferation by neurotransmitters in the developing vertebrate retina. *Brain Res.* **1192**, 37-60.
Massé, K., Bhamra, S., Eason, R., Dale, N. and Jones, E. A. (2007). Purine-mediated signalling triggers eye development. *Nature* **449**, 1058-1062.
Nasmyth, K. (1996). Viewpoint: putting the cell cycle in order. *Science* **274**, 1643-1645.
Nuckels, R. J. and Gross, J. M. (2007). Histological preparation of embryonic and adult zebrafish eyes. *Cold Spring Harbor Protocols*, doi:10.1101/pdb.prot4846
O'Donnell, A. F., Tiong, S., Nash, D. and Clark, D. V. (2000). The Drosophila melanogaster ade5 gene encodes a bifunctional enzyme for two steps in the de novo purine synthesis pathway. *Genetics* **154**, 1239-1253.
Pearson, R., Catsicas, M., Becker, D. and Mobbs, P. (2002). Purinergic and muscarinic modulation of the cell cycle and calcium signaling in the chick retinal ventricular zone. *J. Neurosci.* **22**, 7569-7579.
Pearson, R. A., Dale, N., Llaudet, E. and Mobbs, P. (2005). ATP released via gap junction hemichannels from the pigment epithelium regulates neural retinal progenitor proliferation. *Neuron* **46**, 731-744.
Rawls, J. M. and Fristrom, J. W. (1975). A complex genetic locus that controls the first three steps of pyrimidine biosynthesis in Drosophila. *Nature* **255**, 738-740.
Spiegel, E. K., Colman, R. F. and Patterson, D. (2006). Adenylosuccinate lyase deficiency. *Mol. Genet. Metab.* **89**, 19-31.
Stone, R. L., Aimi, J., Barshop, B. A., Jaeken, J., Van den Berghe, G., Zalkin, H. and Dixon, J. E. (1992). A mutation in adenylosuccinate lyase associated with mental retardation and autistic features. *Nat. Genet.* **1**, 59-63.
Sugioka, M., Zhou, W.-L., Hofman, H.-D. and Yamashita, M. (1999). Involvement of P2 purinoceptors in the regulation of DNA synthesis in the neural retina of chick embryo. *Int. J. Dev. Neurosci.* **17**, 135-144.
Thisse, B. and Thisse, C. (2004). Fast release clones: a high throughput expression analysis. *ZFIN Direct Data Submission* (http://zfin.org).
Tiong, S. Y., Keizer, C., Nash, D., Bleskan, J. and Patterson, D. (1989). Drosophila purine auxotrophy: new alleles of adenosine 2 exhibiting a complex visible phenotype. *Biochem. Genet.* **27**, 333-348.
Uribe, R. A. and Gross, J. M. (2007). Immunohistochemistry on cryosections from embryonic and adult zebrafish eyes. *Cold Spring Harbor Protocols*, doi:10.1101/pdb.prot4779
Willer, G. B., Lee, V. M., Gregg, R. G. and Link, B. A. (2005). Analysis of the zebrafish perplexed mutation reveals tissue-specific roles for de novo pyrimidine synthesis during development. *Genetics* **170**, 1827-1837.
Zalkin, H. and Dixon, J. E. (1992). De novo purine nucleotide biosynthesis. *Prog. Nucleic Acids Res. Mol. Biol.* **42**, 259-287.
Ziegler, I. (2003). The pteridine pathway in zebrafish: regulation and specification during the determination of neural crest cell-fate. *Pigment Cell Res.* **16**, 172-182.
Zollner, N. (1982). Purine and pyrimidine metabolism. *Proc. Nutr. Soc.* **41**, 329-342.